

Diaphyseal intramedullary osteoid osteoma: an enigmatic subtype

M. F. MOSTAFA¹, S. I. FAWZY¹, K. R. ZALATA²

¹Department of Orthopaedics and Traumatology, Orthopaedic Oncology Unit, Mansoura University Hospital, Mansoura, Egypt; ²Department of Pathology, Mansoura University, Mansoura, Egypt.

Correspondence at: Mohamed F. Mostafa, Mansoura University Hospital, 36 Al-Gomhoria Street, P. O. Box 35516, Mansoura, Egypt.
E-mail: thabetortho20032003@yahoo.com

ABSTRACT This retrospective study aimed to evaluate patients with similar clinical and radiological features of diaphyseal intramedullary osteoid osteoma, an enigmatic location subtype.

Sixteen patients (11 males and 5 females) with an average age of 12.3 years at the time of presentation were reviewed. The lesion was located in the tibia unilaterally in 10 patients, bilaterally in three, and in the femur unilaterally in three. Diagnosis was established based on the typical clinical presentation of OO and the identification of nidus on computed tomography (CT) scan and magnetic resonance imaging (MRI), and confirmed by histopathological examination of tissues obtained during surgery. All patients underwent en bloc excision of the intramedullary abnormal bone, including the nidus, through a small cortical window.

The typical pain of OO was the main complaint in all patients and was completely relieved by the second day after surgery. Out of the 16 histopathologically confirmed lesions, 15 showed a visible nidus on CT scan and MRI. After a mean follow-up period of 40.1 months (range 26 – 73 months), most patients were enthused about surgery and resumed their daily activities without pain or any limitation of movement. Only one patient experienced a traumatic tibial fracture at the operative site 3 months after surgery and healed spontaneously after 6 weeks of immobilization.

Diaphyseal intramedullary osteoid osteoma should be considered when the typical clinical picture is present, regardless of whether the nidus is detected radiologically.

Keywords: Osteoid osteoma, diaphyseal, intramedullary.

INTRODUCTION

Osteoid osteoma is a common osteoblastic benign bone tumor that was first described in 1930 by Bergstrand¹ and recognized later on as a unique entity by Jaffe in 1935². It is a small painful lesion characterized by an osteoid-rich nidus less than 2 cm in size, showing variable degrees of central mineralization and surrounded by reactive bone sclerosis³. It accounts for approximately 5% of all primary bone tumors and 11% of benign bone tumors⁴. Osteoid osteoma affects most frequently adolescents and young adults, with a male preponderance⁵. The classic presentation is throbbing or nagging bone pain localized to the site of the lesion that worsens at night and is dramatically relieved with salicylates or non-steroidal anti-inflammatory drugs (NSAIDs). This characteristic pain is so common as to be diagnostic of OO in the majority of patients⁶.

The location of OO within the long tubular bones may vary. Although the classic and most common location is within the cortex, subperiosteal and intramedullary involvement have been reported^{7,8}. Intramedullary OO is referred to in the literature as cancellous or metaphyseal OO and is relatively infrequent. This lesion is typically located in the long bone metaphysis, femoral neck, and carpal and tarsal bones. The little reactive new bone formation about the nidus and the extensive perilesional marrow edema give these lesions a different overall appearance from the more common cortical lesions and make subsequent diagnosis challenging⁹. The occurrence of intramedullary OO in the diaphysis of long bones is rare, and only a few cases have been reported¹⁰⁻¹³. Moreover, diagnosing diaphyseal intramedullary OO is more difficult and usually requires histopathological confirmation⁸. Differential diagnoses of these cases include conditions that induce intramedullary sclerosis, such as chronic multifocal sclerosing osteomyelitis,

intramedullary osteosclerosis, Ribbing disease, Camurati-Engelmann disease, Erdheim-Chester disease, and Hardcastle syndrome¹⁴. Because of the rarity of diaphyseal intramedullary OO, it is difficult to report a large series of such patients in one study.

The current study was conducted to evaluate the clinical and radiological features of a group of patients with diaphyseal intramedullary OO, which represents an enigmatic location subtype of the tumor.

MATERIALS AND METHODS

We retrospectively reviewed the records and radiographs of all patients with OO who were managed at our institution between January 2010 and December 2019. A total of 126 patients with osteoid osteoma were detected (intracortical=82, intramedullary=36, subperiosteal=2, spine=2, and pelvis=4). Patients of any age with an intramedullary lesion confined to the diaphysis of a long bone between the square area of proximal and distal metaphysis and the endosteum of intact cortex were selected. Sixteen patients with a diagnosis of diaphyseal intramedullary OO were available. All patients were managed in the same way by the same authors. Informed consent was obtained from patients or their relatives that data of clinical presentation, radiological findings, operative details,

and follow-up would be submitted for publication. There were 11 males and 5 females with an average age of 12.3 years (range 4 – 30 years) at the time of presentation (Table I). The lesion was located intramedullary in the diaphysis of the tibia unilaterally in 10 patients (56.3%), tibia bilaterally in 3 (25%), and femur unilaterally in 3 (18.8%). Insignificant trauma to the affected limb was reported by 6 patients. One patient (Case 6) with bilateral tibial lesions had a traumatic fracture of the right tibia and a failed trial of open excision on the left side. Two more patients with femoral lesions had failed trials to excise the lesion by medullary reaming in one and percutaneous radiofrequency ablation in the other.

Pain was the main complaint in all patients and was associated with limping in four patients and even inability to bear weight on the affected limb in two more patients. The pain was typically deep, boring, and localized to the site of the lesion. It was worse at night and partially relieved with non-steroidal anti-inflammatory drugs. Restlessness, inability to sleep at night, and decreased use of the affected limb were noted by parents of young children. Before surgery, all patients reported intolerance and persistence of pain despite medication. The mean duration of symptoms was 6 months (range 3 – 10 months). The local signs of swelling, warmth, and tenderness were evident

Table I. — Details and results in 16 patients with diaphyseal intramedullary OO.

No	Age (years)	Gender	location	Symptoms (months)	Nidus on CT		Nidus on MRI		Sclerosis	Previous surgery	Histological confirmed	Complications	Follow-up (months)
					R	L	R	L					
1	12	F	Tibia bilat	6	+	+	Ring	Ring	-	-	+	-	73
2	5	M	Tibia unilat	3	Not	+	Not	Target	+	-	+	-	64
3	11	F	Tibia bilat	7	-	+	-	Ring	+	-	+	-	60
4	7	F	Tibia unilat	5	+	Not	Bell	Not	-	-	+	-	50
5	7	M	Femur	4	+	Not	Ring	Not	+	+	+	-	47
6	10	M	Tibia bilat	6	-	+	Ring	Target	+	+	-	Fracture	46
7	4	M	Tibia unilat	3	+	Not	Bell	Not	+	-	+	-	40
8	30	M	Tibia unilat	10	Not	+	Not	Ring	-	-	+	-	35
9	17	M	Femur	8	Not	+	Not	Target	+	+	+	-	30
10	16	M	Tibia unilat	8	Not	+	Not	-	+	-	-	-	30
11	11	F	Tibia unilat	6	+	Not	Ring	Not	-	-	+	-	28
12	16	M	Tibia unilat	7	Not	+	Not	Target	+	-	+	-	27
13	8	M	Femur	6	+	Not	Target	Not	+	-	+	-	26
14	15	M	Tibia unilat	8	+	Not	Target	Not	-	-	+	-	32
15	10	F	Tibia unilat	4	+	Not	Target	Not	-	-	+	-	28
16	18	M	Tibia unilat	5	Not	+	Not	Ring	+	-	+	-	26

+ present; - absent; Not; not involved.

in six patients with tibial lesions. The inflammatory markers were slightly elevated in those cases. This made the diagnosis of OO more difficult because of the increased possibility of infection. Only one patient (Case 7) with tibial OO presented with valgus deformity of the knee and limb lengthening.

Plain radiographs and computed tomography of all patients were reviewed for the presence of abnormal diaphyseal intramedullary sclerosis, visible nidus within the sclerotic area, and the extent of cortical sclerosis and thickening (Figure 1). Additionally, MRI, particularly the contrast-enhanced axial images, was evaluated to detect the nidus within the medullary lesion. The location of the lesion inside the medulla was determined on axial CT scan and MRI by constructing external and internal cortical lines continuous with those on either side of the lesion (Figure 2). The nidus was detected by the presence of a target-like, bell, or ring appearance, especially if it coincides in location with that on CT images. In the typical target-like appearance, the central area of low signal intensity represents the mineralized portion of the nidus, while the high signal intensity at the periphery represents the unmineralized portion of the nidus surrounded by the low signal intensity of the abnormal intramedullary reactive bone (Figure 3a). Presence of the mineralized part to the side of

the nidus gave the bell appearance (Figure 3b), and absence of this part gave the ring appearance (Figure 3c). The high signal intensity on T2-weighted images caused by edema in the adjacent bone marrow and soft tissues made localization of the nidus difficult and misled to more aggressive lesion. Technetium 99-m methylene diphosphonate bone scintigraphy was available for 12 patients. The increased perfusion and delayed focal intense uptake help to confirm the diagnosis, localize the lesion to the bone diaphysis, and detect bilateral lesions.

Operative technique

Surgery was performed under general anesthesia in 11 patients and spinal anesthesia in 5. A thigh tourniquet was used for patients with tibial lesions to reduce intraoperative bleeding and to improve visualization. To localize skin incision over the lesion, the proximal and distal extents of the intramedullary sclerosis were marked on the skin preoperatively, guided by an image intensifier. The lateral approach was used for femoral lesions, while tibial lesions were approached directly from the anteromedial aspect. The periosteum was incised longitudinally along the skin incision and retracted on each side to expose the underlying bone. In most patients, the outer cortex showed an area of purple discoloration and oozed



Fig. 1 — Anteroposterior (a) and lateral (b) radiographs of the left leg (case 1) show diaphyseal intramedullary sclerosis. Coronal (c) and axial (d) CT scans confirm the presence of abnormal intramedullary bone with a visible nidus on axial cut.

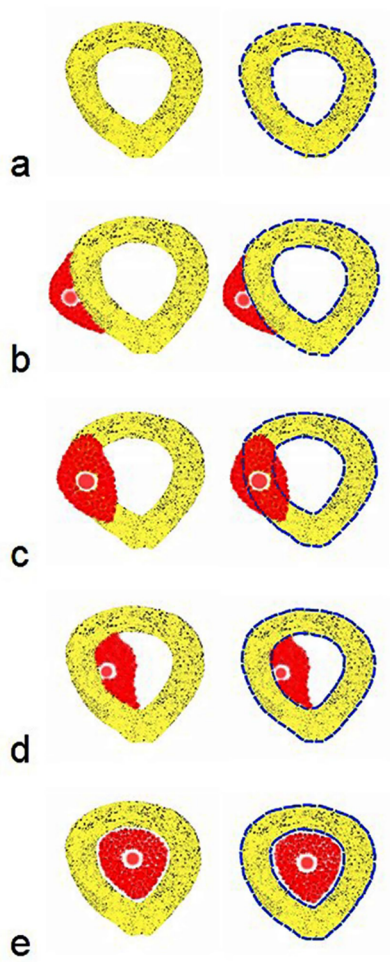


Fig. 2 — Drawings show how the location of osteoid osteoma is determined. (a) Cross-section of normal long tubular bone with the dotted blue lines marking the outer and inner cortex. (b-e) Show the location of the nidus in relation to the dotted lines, and the stippled red areas represent new bone formation associated with the nidus. (a) Normal bone, (b) Subperiosteal, (c) Cortical, (d) Intramedullary (endosteal or eccentric) and (e) Intramedullary (medullary or centric).

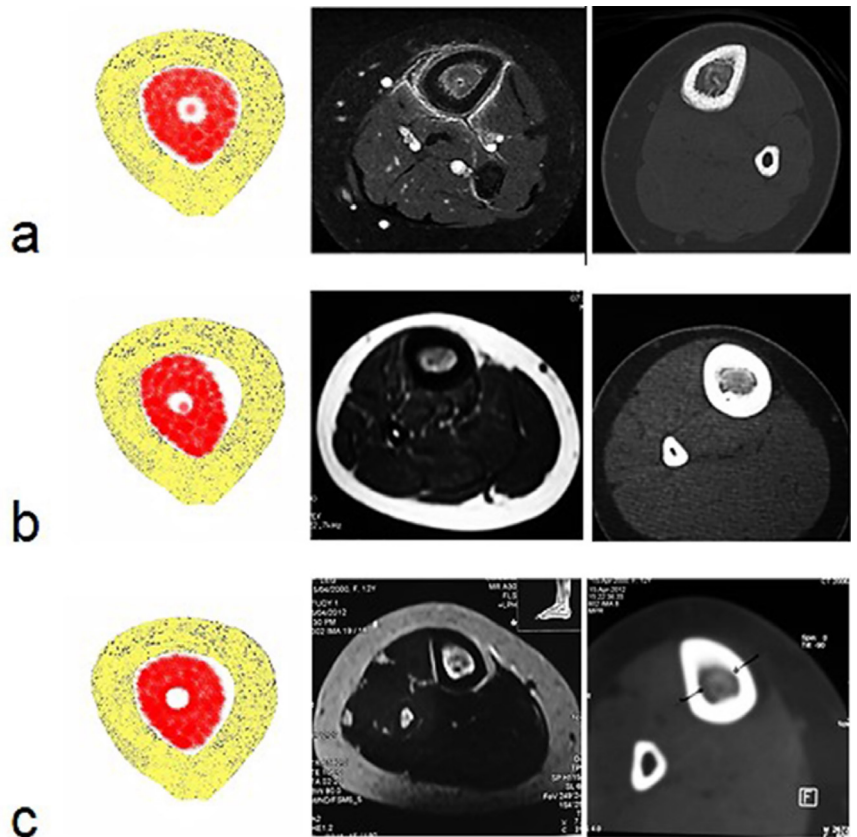


Fig. 3 — Drawings of long bone cross-section, axial MRI, and corresponding CT cuts of tibial lesions. (a) The mineralized central portion of the nidus gives the typical target appearance (case 12). (b) The location of the mineralized portion to the side of the nidus gives the bell appearance (case 4). (c) Absence of a mineralized portion gives the ring appearance of the nidus (case 1).

blood at the level of the lesion, where the medulla contained the abnormal and highly vascularized trabecular bone. A small rectangular-shaped cortical window with rounded angles was made. The length of the window was determined by the extent of the intramedullary sclerosis, while the width was planned not to exceed half the diameter of bone at the level of surgery to avoid the stress riser effect. Multiple drill holes at 5 mm intervals were made along the marked area of the cortical window using a 2.5 mm drill bit. The holes were then connected with a small osteotome, and the cortical window was removed

to expose the underlying medulla. The abnormal intramedullary bone trabeculae, including the nidus, were carefully curetted, excised into one piece, and sent for histopathological examination. A sample of the excised tissue was obtained for culture and sensitivity test in cases suspected to have infection. After clearing the medullary canal, periosteal edges were approximated with interrupted sutures, and the wound was closed in layers.

Postoperatively, the limb was splinted in a removable and well-padded brace for 6 weeks. During this period, patients were mobilized non-

weight bearing and asked to move joints and toes out of the brace 3 to 4 times daily. Thereafter, they were allowed partial weight bearing, progressing to full weight bearing guided by clinical and radiological healing. All patients were evaluated clinically and radiologically using plain radiographs every month for the first 6 months after surgery, every 3 months for the next 1.5 years, then yearly, and at the time of final follow-up. Follow-up CT scan and bone scintigraphy were requested for most of the patients after completing one year from surgery.

All patients were asked about complete relief or persistence of pain on the second day postoperatively and recurrence or development of pain at other sites on follow-up. Clinical assessment was done for surgical wound complications, angular deformity or limb length discrepancy, and limitation of nearby joint movement. The occurrence of a fracture through the operative site was also reported. Plain radiographs were evaluated for completeness of removal of the intramedullary lesion, healing of the cortical window, and the progress of limb deformity. The follow-up CT scan and bone scintigraphy performed one year after surgery were reviewed to ensure complete eradication of the tumor.

RESULTS

The typical pain of OO was present preoperatively in all patients and completely relieved by the second day after surgery. The average time to develop pain in the other limb in patients with bilateral lesions was 6.8 months (range 2 – 18 months). There were no patients with recurrence of pain after surgical excision of the lesion. The abnormal diaphyseal intramedullary sclerosis was detected on plain radiographs of the 19 lesions included, with a clearly detectable nidus in 12 (60%) of them. The nidus was visible on CT scan and MRI in 17 (90%) lesions. On MRI, particularly the contrast-enhanced axial views, the nidus appeared as a typical target in 7 lesions, atypical bell in 2, and atypical ring in 8. Reactive sclerosis or thickening of the outer cortex was detected on plain radiographs and CT scans in 10 patients (12 lesions; 9 tibias and 3 femurs). All patients with a history of insignificant trauma to the affected limb had reactive sclerosis and cortical thickening at the time of presentation. Preoperative radiographs were misinterpreted as Ewing's sarcoma in 3 patients and chronic osteomyelitis in 7.

The tissue excised from the medulla was highly vascular cancellous bone trabeculae and not compact bone. The medulla seemed to be plugged

with cancellous bone where it should be clear of bone and filled with bone marrow. The nidus tissue could be detected grossly within the intramedullary cancellous bone in only three lesions. Diagnosis of OO was confirmed histopathologically in 16 (84%) lesions (13 tibias and 3 femurs) by the presence of an interlacing network of bone trabeculae with different levels of mineralization and a highly vascular stroma of connective tissue. The trabeculae were rimmed with active plump osteoblasts and accompanied by numerous osteoclast-like multinucleated giant cells (Figure 4). The remaining 3 (15%) tibial lesions did not show this typical microscopical picture. One patient (Case 6) with bilateral tibial lesions revealed thick bone trabeculae and intervening fibrovascular stroma. This patient had a failed trial of surgical excision of the left lesion and a healed traumatic fracture close to the right lesion. The other patient showed a picture of chronic non-specific osteomyelitis. Most patients (92.3%) with no previous surgical trial to excise the lesion had a histopathologically confirmed diagnosis of OO. Out of the 16 lesions that were histopathologically confirmed, 15 (93.8%) had a visible nidus on CT scan and MRI. Among the three lesions that were not histologically confirmed, the nidus could not be detected on CT scan in one lesion (right side of a bilateral tibial patient) and on MRI in one more lesion (unilateral tibial patient).

The patients were followed up for a mean duration of 40.1 months (range 26–73 months). At the time of final follow-up, most patients were enthused by the surgery and resumed their daily activities without pain or any limitation of movement of the nearby joint. There were no cases of surgical wound complications. Only one patient developed a traumatic tibial fracture at the operative site 3 months after surgery and healed spontaneously by immobilization for 6 weeks. This patient had a failed trial to excise the lesion at a referral hospital. The patient who presented with valgus knee and limb lengthening preoperatively was managed by guided growth surgery to control deformity and to improve the way of walking. Follow-up radiographs and bone scintigraphy revealed complete eradication of the tumor. The CT scan performed one year after surgery showed complete healing of the cortical window and restoration of cortical continuity.

RESULTS

OO is a small benign osteoblastic tumor that affects mainly pediatric and young adult populations, constituted by osteoid bone microtrabeculae and

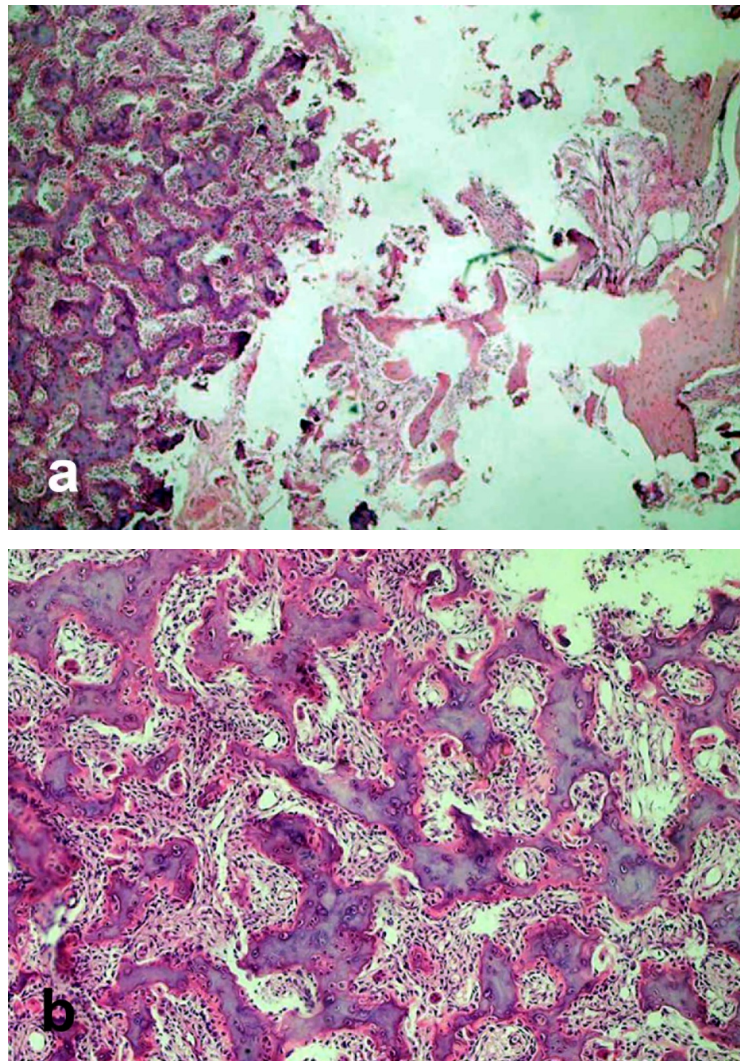


Fig. 4 — (a) Low-power histological section shows the lace-like nidus of osteoid osteoma surrounded by bone. (b) The tumor consists of an interlacing network of woven bone trabeculae rimmed with active osteoblasts and a highly vascular connective tissue stroma containing numerous osteoclast-like multinucleated giant cells.

circumscribed by sclerotic bone tissues. It presents clinically with disproportionate pain that initially occurs intermittently at night and is generally responsive to non-steroidal anti-inflammatory drugs in 80% of patients¹⁵. OO is cortically based and consists of a radiolucent nidus with a surrounding area of reactive sclerotic bone that usually can be seen on radiographs. Any bone can be affected, but the femur and tibia account for more than half of the cases, and the proximal femur for almost one-third¹⁶. In long tubular bones, OO is more often situated in the corticodiaphyseal or metaphyseal regions. Other locations, such as intramedullary, subperiosteal, epiphyseal, or apophyseal, have also been reported¹⁷.

In 1966, Edeiken et al.¹⁸ categorized three types of OO based on radiographic localization of the nidus:

cortical (within the cortex), subperiosteal (on the external aspect of the cortex), and intramedullary (within the medulla). The intramedullary location was noted to be within the cancellous bone of the long bone metaphysis. Consequently, OO was classified as cortical, cancellous, and subperiosteal¹⁹. Kayser et al.⁷ reported the subperiosteal origin of OO and concluded that cortical, endosteal, and intramedullary locations could result from continuous bone remodeling with subperiosteal deposition and endosteal resorption. The presence of OO inside the medulla of long bone diaphysis is rare and only reported sporadically as a case presentation¹⁰⁻¹³. To the authors' knowledge, a large series of these atypically located osteoid osteomas has not been reported in the literature. We report 16 patients with 19 intramedullary diaphyseal OO of the tibia and

femur. This leads to the suggestion that intramedullary OO can be metaphyseal and diaphyseal. Metaphyseal intramedullary OO often fails to elicit a reactive bone formation or intense periosteal reaction²⁰. On the other hand, diaphyseal intramedullary OO may be associated with intense reactive bone sclerosis¹⁰. All cases included in our study had an abnormal intramedullary trabecular bone and reactive sclerosis of the adjacent cortex in 12 lesions.

The atypical location of the lesion within the medulla of long bone diaphysis poses a diagnostic challenge. However, the typical clinical presentation and identification of the nidus on CT scan and MRI established the diagnosis of OO. A CT scan is generally preferred to MRI in delineating the small lucent nidus surrounded by reactive bone²¹. When the lesion is located in the cancellous bone, a CT scan may fail to identify the nidus due to the lack of perinidal bone sclerosis²². Visualizing the nidus by MRI can be difficult because the signal intensity in the nidus is often similar to that of the surrounding bone sclerosis. Moreover, bone marrow and soft tissue edema may produce a misleading aggressive appearance^{21,23}. Recent studies have shown that MRI performed with techniques to increase spatial resolution and contrast enhancement may be equally as effective as or more effective than CT for detecting the nidus with greater conspicuity. This is particularly true for intramedullary locations²⁴. In the current study, MRI was highly suggestive for diagnosing OO in addition to CT scan. The nidus was visible in 17 (90%) lesions, particularly on contrast-enhanced axial MRI, 15 (88%) of them were histologically confirmed.

While the main differential diagnosis of metaphyseal OO is Brodie's abscess²⁵, the differential diagnosis of diaphyseal intramedullary OO includes conditions that induce intramedullary bone formation, such as Camurati-Engelmann disease, intramedullary osteosclerosis, chronic multifocal sclerosing osteomyelitis, Hardcastle syndrome, and Ribbing disease¹⁴. In the current study, 3 patients were initially misdiagnosed radiologically as Ewing's sarcoma and 7 as chronic osteomyelitis.

Pre-operative CT-guided or open incisional biopsy was recommended by many authors to confirm the diagnosis, especially for metaphyseal lesions^{25,26}. However, others preferred to do an excision biopsy considering the typical presentation of OO and the absence of malignant features such as permeative bone destruction, endosteal scalloping, or associated soft tissue component^{8,11,12}. Despite the unusual intramedullary location of the lesion, pre-operative biopsy was not required for our cases. The consistent

clinical and radiological diagnosis of OO and the absence of any evidence of malignancy encouraged excision biopsy. This allowed an adequate tissue sample for histopathological examination and identification of the nidus, helping to confirm diagnosis and to ensure complete excision. Although conservative management with prolonged use of non-steroidal anti-inflammatory analgesics may be effective, the possible skeletal and renal complications limit its application as a definitive treatment in young patients²⁷. In the current study, pain associated with diaphyseal intramedullary OO seemed to be more intense than that with cortical lesions. The severity and persistence of pain despite medication force the patients to undergo surgery.

Until recently, complete surgical excision with curettage or en bloc resection has been the treatment of choice to relieve pain with a low recurrence rate^{19,28}. Less invasive techniques utilizing pinpoint CT-guided localization have been introduced to reduce the potential morbidity seen with traditional open techniques, especially for difficult-to-reach lesions. Several studies reported good to excellent results after percutaneous CT excision of the lesion using a biopsy punch, trephine, or core drill over a Kirshner wire inserted into the nidus. Despite the high success rate of these techniques, there was a significant risk of incomplete excision of the nidus and recurrence of pain necessitating more surgery. Furthermore, the tissue sample obtained is usually inadequate for histological examination²⁹.

Rosenthal et al.³⁰ in 1992 described the technique of radiofrequency thermal ablation (RFTA) for the treatment of OO and currently become the treatment of choice for extra-spinal lesions in both adult and pediatric patients. Image-guided percutaneous interstitial laser photocoagulation, microwave ablation, and cryoablation are other minimally invasive techniques for managing osteoid osteoma with a high primary clinical success rate of 90-100% and complication rate of 5-14%³¹⁻³³. Falappa et al.³⁴ treated three patients of tibial metaphyseal intramedullary OO with cold mode RFTA and concluded that the technique is minimally invasive and safe with a high clinical success rate. However, inaccurate needle placement, particularly in small diameter nidus, and the development of hyperthermia that limits heating duration were found to be the main causes of the frequent treatment failure and the need for a second ablation session³⁵. Although this minimally invasive RFTA technique is regularly performed in our institution, it could require general anesthesia in young patients. Therefore, we preferred to proceed with open excision of such atypically

located lesions. It is believed that complete removal of the nidus will result in immediate and maintained pain relief. Moreover, the obtained tissue will be sufficient to confirm the diagnosis and to ensure complete eradication of the tumor. Rouhani et al.¹¹ managed two adult patients with tibial intramedullary OO by medullary reaming through a small trans-patellar tendon approach. They noted that the technique is simple, safe, and cost-effective allowing early return to weight-bearing and recreation activities without risk of fracture. However, the main drawback of this method is the loss of histopathological confirmation of diagnosis. Intramedullary reaming failed to relieve pain in one patient with a femoral lesion in our study (Case 9). Also, this technique looked impractical for children and adolescents because of the risk of proximal tibial physeal injury in tibial cases and the femoral head vascularity affection in femoral cases. The current is not free of limitations. The relatively small sample size and the retrospective nature of the study may have inherent bias in our results. The heterogeneous materials regarding the location of the lesion and the age of patients confound the results and make it difficult to obtain statistical significance. The lack of a control group managed by the commonly used radiofrequency thermal ablation reduces the strength of the study.

CONCLUSION

Diaphyseal intramedullary OOs are relatively uncommon and pose a diagnostic challenge due to the unusual location of the lesion and the confusing radiological features. Intramedullary OOs are often misdiagnosed as Ewing's sarcoma and osteomyelitis; however, the typical clinical presentation and identification of the nidus on CT scan and MRI are helpful to set the diagnosis of OO. Despite the limited number of patients, the authors suggest adding diaphyseal intramedullary OO as a location subtype. In this way, intramedullary OO can be metaphyseal or diaphyseal. Although minimally invasive techniques can be successful in eliminating pain, complete surgical excision of the intramedullary bone, including the nidus, is the preferred treatment for such atypically located lesions. This will allow permanent pain relief, histological confirmation of diagnosis, and complete eradication of the lesion.

Conflict of Interest: The authors declare that they have no conflict of interest.

Funding: No funds, grants, or other support were received.

Ethical Approval: The local ethics committee of Medical

College, Mansoura University, waived ethical approval in view of the retrospective nature of the study, and all the procedures performed were part of routine care.

Informed consent: Informed consent was obtained from patients or their guardians to participate in this study.

Acknowledgement: There is no acknowledgement.

REFERENCES

1. Bergstrand H. Uber eine eigenartige, wahrscheinlich bisher nicht beschriebene osteoblastische Krankheit in den langgen Knochen in der Hand und des Fusses. *Acta Radiol.* 1930; 11: 596-613.
2. Jaffe HL. Osteoid osteoma: A benign osteoblastic tumor composed of osteoid and atypical bone. *Arch Surg.* 1935; 31: 709-728.
3. Resnick D, Kyriakos M, Greenway GD. Tumors and tumor-like lesions of bone: imaging and pathology of specific lesions. In: Resnick D, Kransdorf MJ (eds). *Bone and joint imaging*, 3rd ed. Saunders, Philadelphia, PA, 2005; pp 1120-1130.
4. Lee EH, Shafi M, Hui JH. Osteoid osteoma: a current review. *J Pediatr Orthop.* 2006; 26 (5): 695-700.
5. Campanacci M. *Bone and Soft Tissue Tumors.* Springer-Verlag, Wien, New York, 1999; pp 391-414.
6. Frassica FJ, Waltrip RL, Sponseller PD, Ma LD, McCarthy EF. Clinicopathologic features and treatment of osteoid osteoma and osteoblastoma in children and adolescents. *Orthop Clin North Am.* 1996; 27 (3): 559-74.
7. Kayser F, Resnick D, Haghghi P, Pereira E do R, Greenway G, Schweitzer M, Kindynis P. Evidence of subperiosteal origin of osteoid osteoma in tubular bones: analysis by CT and MRI imaging. *Am J Roentgenol.* 1998; 170 (3): 609-14.
8. Halanski MA, Mann DC. Case report: unusual tibia intramedullary osteoid osteoma in a two-year-old. *Iowa Orthop J.* 2005; 25: 66-8.
9. Kransdorf MJ, Murphey MD. Osseous tumors. In: Davies AM, Sundaram M, James SL, (eds). *Imaging of bone tumors and tumor-like lesions. Techniques and applications.* Berlin, Heidelberg: Springer-Verlag; 2009: 251-304.
10. Jawish R, Kassab F, Kairallah S, Rizk R. Osteoid osteoma of the intramedullary diaphyse in children. *Rev Chir Orthop Reparatrice Appar Mot.* 1997; 83 (1): 74-7.
11. Rouhani AR, Najafi A, Rouhani S. Excision of osteoid osteoma with intramedullary reaming: a new method. *Acta Med Iran.* 2011; 49 (4): 265-8.
12. Gupta S, Sinha S, Narang A, Kanojia RK. Intramedullary osteoid osteoma in an 11-month-old child. *J Postgrad Med.* 2020; 66 (1): 57-58.
13. Hiramatsu M, Nakayama R, Kasahara T, Nakagawa R, Hirozane T, Yamaguchi S, Mori T, Asano N, Okita H, Nakamura M, Matsumoto M. Intramedullary osteoid osteoma in the humerus of a toddler-A case report and review of the literature. *Radiol Case Rep.* 2022; 17 (10): 3748-53.
14. Kang S, Han I, Shin SH, Kim H-S. Orthopedic case of the month: lower leg pain in a 41-year-old woman. *Clin Orthop Relat Res.* 2012; 470 (1): 321-6.
15. Fletcher CDM, Bridge JA, Hogendoorn PCW, Mertens F, (eds). *World Health Organization (WHO) classification of tumors of soft tissue and bone*, 4th ed. Lyon, France: IARC, 2013; pp 277-8.
16. Cohen MD, Harrington TM, Ginsburg WW. Osteoid Osteoma: 95 cases and review of the literature. *Semin Arthritis Rheum.* 1983; 12 (3): 265-81.
17. Ghanem I. The management of osteoid osteoma: updates and controversies. *Curr Opin Pediatr.* 2006; 18 (1): 36-41.

18. Edeiken J, DePalma AF, Hodes PJ. Osteoid osteoma (Roentgenographic emphasis). *Clin Orthop Relat Res.* 1966 Nov-Dec; 49: 201-6.
19. Kitsoulis P, Mantellos G, Vlychou M. Osteoid osteoma. *Acta Orthop Belg.* 2006; 72 (2): 119-25.
20. Klein MH, Shankmann S. Osteoid osteoma: radiologic and pathologic correlation. *Skeletal radiol.* 1992; 21 (1): 23-31.
21. Assoun J, Richardi G, Railhac JJ, Baunin C, Fajadet P, Giron J, et al. Osteoid osteoma: MR imaging versus CT. *Radiology.* 1994; 191 (1): 217-23.
22. Hosalkar HS, Garg S, Moroz L, Pollack A, Dormans JP. The diagnostic accuracy of MRI versus CT imaging for osteoid osteoma in children. *Clin Orthop Relat Res.* 2005 Apr; 433: 171-7.
23. Hayes CW, Conway WF, Sundaram M. Misleading aggressive MR imaging appearance of some benign musculoskeletal lesions. *Radiographics.* 1992; 12 (6): 1119-34.
24. Liu PT, Chivers FS, Roberts CC, Schuttz CJ, Beauchamp CP. Imaging of osteoid osteoma with dynamic gadolinium-enhanced MR imaging. *Radiology.* 2003; 227 (3): 691-700.
25. Schlur C, Bachy M, Wajfisiz A, Ducou Ie Pointe H, Josset P, Vialle R. Osteoid osteoma mimicking Brodie's abscess in a 13-year-old girl. *Pediatr Int.* 2013; 55 (2): e29-31.
26. Virayavanich W, Singh R, O'Donnell RJ, Horvai AE, Goldsby RE, Link TM. Osteoid osteoma of the femur in a 7-month-old infant treated with radiofrequency ablation. *Skeletal Radiol.* 2010; 39 (11): 1145-9.
27. Carpintero Benitez P, Aguirre MA, Serrano JA, Lluch M. Effect of rofecoxib on pain caused by osteoid osteoma. *Orthopedics.* 2004; 27 (11): 1188-91.
28. Sluga M, Windhager R, Pfeiffer M, Doankus M, Kotz R. Peripheral osteoid osteoma. Is there still a place for traditional surgery? *J Bone Joint Surg Br.* 2002; 84 (2): 249-51.
29. Roger B, Bellin MF, Wioland M, Grenier P. Osteoid osteoma: CT-guided percutaneous excision confirmed with immediate follow-up scintigraphy in 16 outpatients. *Radiology.* 1996; 201 (1): 239-42.
30. Rosenthal DI, Alexander A, Rosenberg AE, Springfield D. Ablation of osteoid osteomas with a percutaneously placed electrode: a new procedure. *Radiology.* 1992; 183 (1): 29-33.
31. Seemann R, Böning G, Schwabe P, Teichgräber U, Gebauer B, Streitparth F. Osteoid osteoma: treatment outcome and long-term follow-up after MRI-guided laser ablation. *Ann Transl Med.* 2022; 10 (5): 240.
32. Parisot L, Grillet F, Verdot P, Danner A, Brumpt E, Aubry S. CT-guided microwave ablation of osteoid osteoma: Long-term outcome in 28 patients. *Diagn Interv Imaging.* 2022; 103 (9): 427-32.
33. Michailidis A, Panos A, Samoladas E, Dimou G, Mingou G, Kosmoliaptsis P, Arvaniti M, Giankoulof C, Petsatodis E. Cryoablation of osteoid osteomas: Is it a valid treatment option? *World J Radiol.* 2024; 16 (9): 389-97.
34. Falappa P, Garganese MC, Crocoli A, Toniolo RM, Lembo A, Marconi F, et al. Particular imaging features and customized thermal ablation treatment for intramedullary osteoid osteoma in pediatric patients. *Skeletal radiol.* 2011; 40 (12): 1523-30.
35. Rosenthal DI, Hornicek FJ, Wolfe MW, Jennings LC, Gebhardt MC, Mankin HJ. Percutaneous radiofrequency coagulation of osteoid osteoma compared with operative treatment. *J Bone Joint Surg Am.* 1998; 80 (6): 815-21.